The Reaction Catalyzed by *Escherichia coli* Aspartate Aminotransferase Has Multiple Partially Rate-Determining Steps, While That Catalyzed by the Y225F Mutant Is Dominated by Ketimine Hydrolysis†

Jonathan M. Goldberg‡ and Jack F. Kirsch*

Department of Molecular & Cell Biology, Stanley Hall, University of California, Berkeley, California 94720-3206

Received September 8, 1995; Revised Manuscript Received January 2, 1996⊗

ABSTRACT: The mechanism of transamination catalyzed by *Escherichia coli* wild-type aspartate aminotransferase (AATase) and the mutant AATase in which Tyr-225 is converted to Phe (Y225F) was investigated. The absorbance spectrum of wild-type AATase in the presence of excess L-Asp and oxalacetate is dominated by species absorbing near 330 nm. The primary C_α ^{2}H-Asp kinetic isotope effects (KIEs) on reactions catalyzed by wild-type AATase at pH 8.9 and 7.5 on k_{cat}/K_M^{Asp} are approximately 2, and the KIEs on k_{cat} are 1.9 (pH 8.9) and 1.4 (pH 7.5). The C_α ^{2}H-Asp KIEs on reactions catalyzed by Y225F are near unity at both pH values. The solvent deuterium KIEs (SKIEs) on k_{cat} for reactions with L-Asp catalyzed by wild-type AATase and Y225F at their pH/pD maxima $\approx$ 2, and the SKIE on k_{cat}/K_M^{Asp} is increased from 1.3 to 2.3 by the mutation. The $C_{4'}$ (*S*)-^{2}H-pyridoxamine 5′-phosphate KIE values on reactions of α-ketoacids with both enzymes are near unity. The viscosity effects on k_{cat}/K_M^{Asp} and k_{cat} for wild-type AATase at pH 9 are 0.10 and 0.31, respectively, indicating that the reaction is partially diffusion limited. The viscosity effects on k_{cat}/K_M^{Asp} and k_{cat} for Y225F are reduced to −0.02 and 0.06, respectively, indicating that the mutant catalyzed reaction is almost fully chemistry-limited. A free-energy profile for the L-Asp-to-oxalacetate half-reaction was constructed for wild-type AATase. C_α H abstraction, ketimine hydrolysis, and oxalacetate dissociation are all partially rate-determining. Ketimine hydrolysis is the sole rate-determining step for the corresponding Y225F-catalyzed reaction.

The mechanism of action of the *Escherichia coli* aspartate aminotransferase is the best understood in the PLP[1] dependent family of enzymes. A detailed mechanism, incorporating newly available structural data and the accumulated spectral and kinetic data, was presented in 1984 (Kirsch *et al*., 1984). Substantial support for the posited roles of the individual amino acids has been advanced by more recent structural investigations of the *E. coli* enzyme and by the results of site-directed mutagenesis studies (Jansonius & Vincent, 1987; Jäger *et al*., 1994; Toney & Kirsch, 1989, 1991; Yano *et al*., 1991, 1993; Cronin & Kirsch, 1988; Hayashi *et al*., 1990; Danishefsky *et al*., 1991; Onuffer & Kirsch, 1994).

The complete process of enzymatic transamination involves at least five kinetically distinguishable steps as shown in Scheme 1. It is not surprising, therefore, that the free energy versus reaction coordinate profile for this enzyme has not yet been quantitatively described completely, although several partial profiles have been published (Fasella & Hammes, 1967; Julin & Kirsch, 1989; Kuramitsu *et al*., 1990; Toney & Kirsch, 1993).

The Y225F mutant has a k_{cat} value equal to 1/450 of that of wild-type enzyme (Goldberg *et al*., 1991). The work described herein explores the question of whether this reduction is due to a change in rate-determining step (or steps) effected by the mutation, or, alternatively to proportional increases in one or more barriers defining the rate-determining step in the wild-type profile. The comparative responses of the wild-type and Y225F mutants to kinetic perturbants, including C_α H and solvent hydrogen isotope effects, and solvent viscosity are combined with spectral data to demonstrate that the mutation changes the free-energy profile from one in which several steps are partially rate-determining to one where ketimine hydrolysis is completely rate-determining. These data and computer simulations were used to construct a free energy versus reaction coordinate profile for the wild-type enzyme that defines quantitatively nearly all of the steps shown in Scheme 1.

MATERIALS AND METHODS

Materials. The wild-type and Y225F mutant forms of AATase were prepared as previously described (Goldberg *et al*., 1991). The N194L mutant form of AATase was a gift from Edward Neymark. C_α ^{2}H-L-Asp was available from an earlier study (Julin & Kirsch, 1989). Other materials were

‡ Present Address: Department of Biochemistry, Beckman Center, Stanford University Medical Center, Stanford, CA 94305-5307.

† This work was supported by NIH Grant Number GM 35393.

⊗ Abstract published in *Advance ACS Abstracts,* March 15, 1996.

[1] Abbreviations: AATase, aspartate aminotransferase (EC 2.6.1.1); PLP, pyridoxal 5′-phosphate; E-PLP, complex of PLP and AATase, also referred to as the internal aldimine; L-Asp, L-aspartate; EL·A, Michaelis complex of E-PLP and L-Asp; EA, Q, and K, the external aldimine, ketimine, and quinonoid intermediates, respectively; PMP, pyridoxamine 5′-phosphate; E-PMP, the complex of AATase and PMP; OAA, oxalacetate; EM·O, the Michaelis of complex of E-PMP and OAA; Y225F, the mutant form of AATase in which Tyr-225 is converted to Phe; N194L, the Asn194 to Leu mutant; αKG, α-ketoglutarate; L-Glu, L-glutamate; αMeAsp, α-methyl-D,L-aspartate; L-CS, L-cysteinesulfinate; MDH, malate dehydrogenase (EC 1.1.1.37); KIE, kinetic isotope effect; SKIE, solvent deuterium KIE; HEPES, *N*-(2-hydroxyethyl)piperazine-*N*′-2-ethanesulfonic acid; MES, 4-morpholineethanesulfonic acid; TAPS, *N*-[tris(hydroxymethyl)methyl]-3-aminopropanesulfonic acid.

0006-2960/96/0435-5280$12.00/0

Scheme 1: L-Asp-to-OAA Half-Reaction Catalyzed by *E. coli* AATase[a]

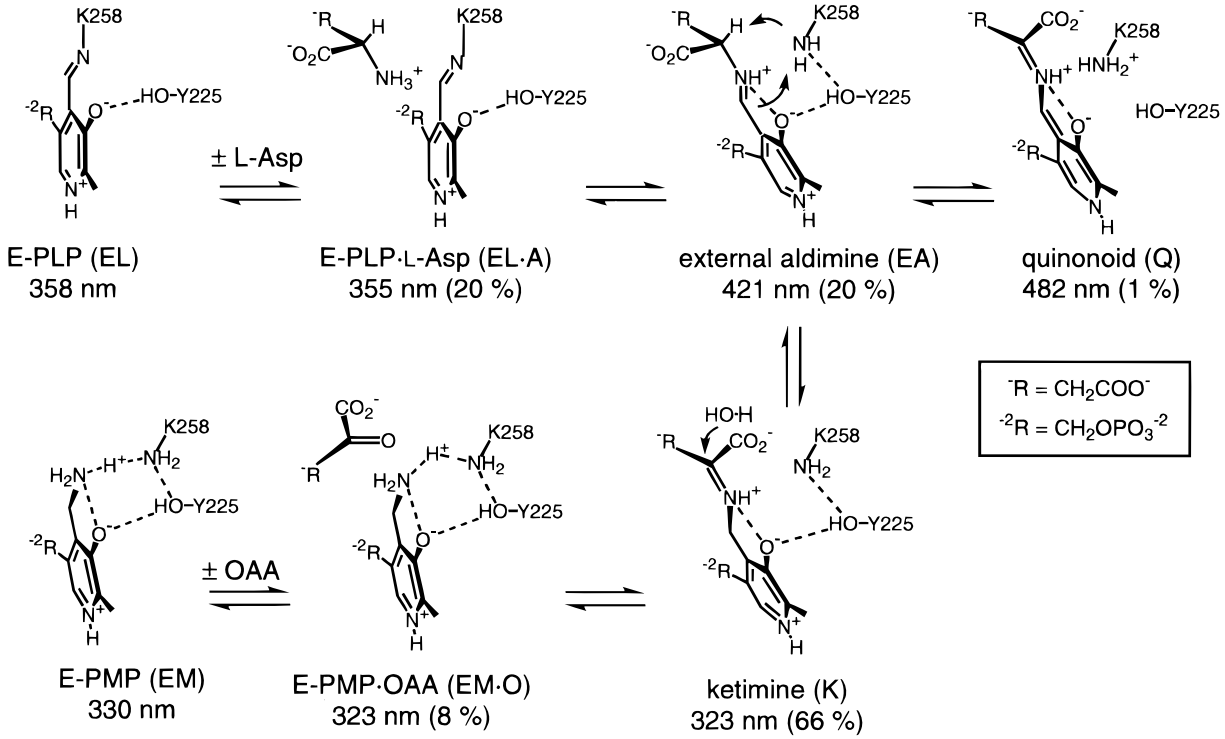

[a] The hydrogen-bonding network and stereochemistry are based on X-ray crystallographic data (Jäger *et al*., 1994). The absorbance maxima of the intermediates are from Table 2. The relative populations of EL·A, EA, and Q are from Table 2, and those of K and EM·O are calculated from the microscopic rate constants in Table 7. The sum of the total population is 115% rather than 100% due to cumulative experimental error.

obtained from standard sources and used without further purification.

Absorbance Spectroscopy. A Kontron UVkon 860 spectrophotometer equipped with a DOS compatible computer and a thermostated circulating water bath was used for spectrophotometric and steady state kinetic measurements. The electronic absorbance spectrum of the AATase−substrate complex was measured at 25 °C in 0.2 M TAPS, pH 8.2, 0.1 M KCl. The concentrations of enzyme, L-Asp, and OAA were 38 μM, 38 mM, and 2 mM, respectively. The SigmaPlot computer program was used to find a set of lognormal distribution functions (Johnson & Metzler, 1970), the sum of which approximated the spectrum of the enzyme−substrate complex.[2] The error estimates for the band parameters are 2% for the well-separated bands at 323 and 421 nm and 4% for the buried bands at 355 and 482 nm (Malashkevich *et al*., 1993).

Primary C_α ^{2}H-Asp Kinetic Isotope Effects. Reactions were initiated by adding L-Asp to solutions containing αKG, 0.4 M TAPS (final pH = 8.90 ± 0.05), and 80 mM KCl (final I_c = 0.2). Final concentrations are in the legend of Figure 2, and T = 25 °C throughout. NADH oxidation was monitored at 340 nm, and runs with protiated and deuterated substrates were alternated. The kinetic parameters at pH 7.5 for the substrates C_α ^{1}H-D,L-Asp and C_α ^{2}H-D,L-Asp were measured as described for L-Asp with [αKG] fixed (Goldberg *et al*., 1991). Concentrations were corrected to account for the nonreactive D-enantiomer.

Solvent Deuterium Kinetic Isotope Effects on Steady State Reactions. Separate αKG/buffer cocktail solutions containing 0.4 M TAPS in H_2O were made for experiments with wild-type AATase and the Y225F mutant. [αKG] = 12 mM and [KCl] = 44 mM for experiments with wild-type AATase. For those with Y225F, [αKG] = 0.2 mM and [KCl] = 80 mM. [KCl] were chosen to obtain I_c = 0.2 after adjustment of the pH or pD. The solutions were adjusted to pH 8.4 (WT) or 9.0 (Y225F), and the volumes were brought to 5 mL in volumetric flasks. The solutions were lyophilized and redissolved in 5 mL of H_2O or D_2O. pH meter readings were corrected for the D_2O effect by adding 0.4 throughout. The pD values of the solutions were 8.8 (WT) and 9.4 (Y225F). Buffer stock solutions containing 0.4 M TAPS and 44 mM KCl (experiments with wild-type AATase) or 80 mM KCl (experiments with Y225F) were prepared by dissolving the components in H_2O or D_2O and adjusting to the appropriate pH or pD by addition of KOH or KOD. Stock solutions containing 200 units of MDH/mL and 20 mM NADH were prepared by diluting a 6000 units/mL stock solution of MDH into the H_2O or D_2O buffer described above and adding solid NADH.

Reactions were performed as follows: 0.4 mL of the buffered αKG/buffer cocktail solution, a variable amount of neutralized L-Asp stock solution, 10 μL of the MDH/NADH cocktail solution, and sufficient H_2O or D_2O to give a final volume of 1 mL were incubated at 25 °C in a cuvette for 4 min, and a blank rate recorded at 340 nm. Reactions were initiated by the addition of 20 μL of the AATase stock solution. The concentration of protium in the final reactions with D_2O was <2%.

pD Titration of the Internal Aldimine. This experiment was carried out as described (Goldberg *et al*., 1991) with the following exceptions: two buffer solutions were prepared in D_2O, one containing 5 mM CHES and 195 mM KCl and adjusted to pD 10.3 with 10 M KOD, and the other

[2] The SigmaPlot spreadsheet and transform used to fit the spectroscopic data are available as supporting information.

containing 100 mM potassium acetate and adjusted to pD 4.2. A 50 μL amount of a 300−500 μM enzyme stock solution was diluted into 1 mL of the CHES buffer, twice concentrated by centrifugal filtration through a 30 kD cutoff filter (Centricon 30), rediluted into the same buffer, and titrated with the acetate buffer. The protium concentration was <5%.

Combined Primary $C_{4'}$ S ^{2}H-PMP and Solvent Kinetic Isotope Effects on Reactions of E-PMP with α-Ketoacids. The complexes of $C_{4'}$ *S* ^{2}H-PMP with wild-type and Y225F AATase were prepared as follows: 100 μL of a 300−500 μM enzyme stock solution was diluted into 0.9 mL of 0.2 M HEPES buffer in D_2O. To the enzyme solution were added 1 μL each of aqueous 60 mM L-CS and 10 mM PMP solutions such that the final concentration of D_2O was 90%. Less than 1% of tritium is transferred from the C_α atom of L-Asp to the $C_{4'}$ atom of the cofactor in single-turnover reactions involving pig cytosolic AATase (Julin & Kirsch, 1989); therefore, the deuterium content of the $C_{4'}$ *pro-S* hydrogen atom of the cofactor reflects the solvent composition. Kochhar *et al*. (1987) have shown that the half-life of tritium on $C_{4'}$ *S* ^{3}H-PMP in *E. coli* AATase is 15 min at pH 7.5 and 25 °C. Thus, the samples were exchanged into buffer containing >98% D_2O by centrifugal filtration through a 30 kDa cutoff filter (Centricon 30) and incubated for 6 h at 4 °C. Deuterium enrichment of PMP at the $C_{4'}$ *pro-S* position was assumed to be complete after 6 h since the washout rate of protium is expected to exceed that of tritium and the temperature difference is expected to reduce the exchange rate only by a factor of approximately 4.

Enzyme and substrate solutions were incubated for 4 min at 25 °C in the reservoirs of an Applied Photophysics 17 MV stopped-flow spectrophotometer. The substrates were 0.1 mM αKG and 0.1 mM OAA for wild-type AATase and Y225F, respectively. Absorbance increases were monitored at 430 nm. In mixed-solvent experiments the enzyme containing $C_{4'}$ *pro-S* ^{1}H-PMP was not exposed to D_2O, and the enzyme containing $C_{4'}$ *S* ^{2}H-PMP was not exposed to H_2O until the reactions were initiated (Scheme 2).

Solvent Viscosity Effects. Steady-state kinetic parameters were determined over a range of sucrose-generated relative viscosities. The reactions contained 0.2 M TAPS (pH 8.4 or 9), 4 units of coupling enzyme (MDH or LDH)/mL and 0.2 mM NADH, and were initiated by adding 10−50 μL of concentrated wild-type AATase, Y225F, or N194L enzyme stock solutions to temperature-equilibrated reaction mixtures. Relative viscosities were determined as described (Bazelyansky *et al*., 1986). Control experiments at high concentrations of wild-type AATase showed that there was sufficient MDH and LDH to couple the reactions over the range of relative viscosities employed.

The dissociation constant of maleate was measured spectrophotometrically as described previously (Goldberg *et al*., 1991) in 0.2 M TAPS, pH 8.4: [wild-type AATase] = 20 μM, [maleate] = 10−250 mM. The K_d value was measured at relative viscosities of 1 and 3.6.

Construction of the Free Energy Profile for the L-Asp-to-OAA Half-Reaction with Wild-Type AATase. A free-energy profile for wild-type AATase was constructed by finding a set of microscopic parameters (eq A1) and intrinsic kinetic isotope effects consistent with the experimentally determined macroscopic parameters collected in Table 6. The experimentally accessible macroscopic parameters were calculated from the microscopic ones with the equations given in Table 1. The kinetic isotope effects on the macroscopic rate constants were calculated from the same equations after substitution of the microscopic rate constants by the ratio of their values and a variable factor (an intrinsic isotope effect > 1).

The calculations required for this simulation were performed with the Microsoft Excel 4.0 application on an Apple Macintosh IIfx computer. The values of the Gibbs free-energy levels of the reaction intermediates and barrier heights, from which the microscopic parameters were calculated with the Eyring equation (Segel, 1993), were varied automatically by the Solver module of Excel until the set of experimentally observed parameters in Table 6

Scheme 2: Protocol for the Deconvolution of the Primary $C_{4'}$ *S* ^{2}H-PMP and Solvent Deuterium Kinetic Isotope Effects (KIEs)[a]

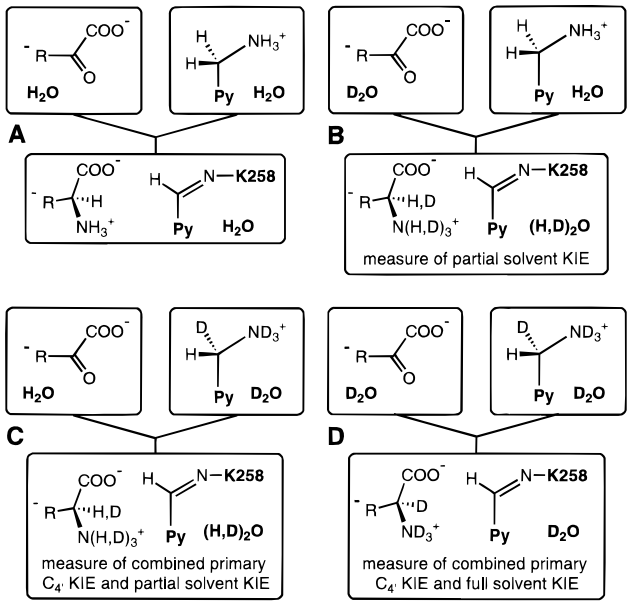

[a] Py denotes the substituted pyridine ring. AATases containing $C_{4'}$ *pro-S* ^{1}H PMP or $C_{4'}$ *S* ^{2}H-PMP AATase were maintained in H_2O or D_2O, respectively, until the initiation of the single-turnover reactions with α-ketoacids in the stopped-flow apparatus in order to prevent isotopic exchange of the $C_{4'}$ *pro-S* atom. The combined full solvent and primary $C_{4'}$ *S* ^{2}H-PMP KIE was determined from a comparison of the kinetics under the conditions diagrammed in experiments A and D. Experiment B gives the partial solvent KIE at a given solvent fraction of D_2O, while experiment C yields the combined partial solvent and primary KIEs at a similar final concentration of D_2O as in B. The difference in the apparent rate constants in experiments C and B, Δk, is a measure of the primary $C_{4'}$ *S* ^{2}H-PMP KIE (see the Discussion).

Table 1: Relationships of Macroscopic Parameters to the Set of Microscopic Rate Constants Defined in Eq A1

k_{cat}/K_M^{Asp}	eq A2
k_{Asp}	eq A3
k_{cat}/K_M^{OAA}	symmetrical with eq A2
k_{OAA}	symmetrical with eq A3
$K_{1,3}$	$([K] + [EM\cdot O])/[EA] = k_{34}/k_{43}(1 + k_{45}/k_{54})$, eq 3b
K_{trans}	K_{eq} for transaldimination: $[EA]/[EL\cdot A] = k_{23}/k_{32}$
normalized solvent viscosity effect on k_{cat}/K_M^{Asp} or k_{cat}/K_M^{OAA}	slope term of eq 1 or A6
normalized solvent viscosity effect on k_{Asp}	slope term of eq A5 × k_{Asp}
normalized solvent viscosity effect on k_{OAA}	symmetrical with the above expression

Table 2: Spectral Analysis of the Substrate-Bound Form of Wild-Type Aspartate Aminotransferase[a]

assignment[b]	band position (nm)	ϵ_0 [c] (M^{-1} cm^{-1})	band width (cm^{-1})	skewness	ref structure	ϵ^{ref}_{max} (M^{-1} cm^{-1})	$\epsilon_0/\epsilon^{ref}_{max}$ [d] (rel population)
protein	275	44000	4650	1.3			
E-PLP·L-Asp (EL·A)	355	1650	4050	1.55	E-PLP[e]	8300[f]	0.20
external aldimine (EA)	421	1650	4400	1.55	E-PLP·H^+[g]	8200[f]	0.20
quinonoid (Q)	482	230	2500	1.8	E-β-HO-Asp[h]	20800[h]	0.011
ketimine and OAA·E-PMP (K and EM·O)	323	6770	4650	1.4	E-PMP[i]	9140[i]	0.74
sum							1.15

[a] Conditions: 38 μM wild-type AAtase, 38 mM L-Asp, 2 mM OAA, 0.2 M TAPS, pH 8.2, 0.1 M KCl, 25 °C. The band parameters in columns 2−5 are from the fit of spectroscopic data between 300 and 550 nm (Figure 1) to summed lognormal distribution functions (see Materials and Methods). [b] The cofactor structures are shown in Scheme 1. [c] Peak height in complex (absorbance/[AATase]). [d] The ratio of the height of the component band (column 3) to that of the extinction coefficient of the reference species (column 7); a measure of that fraction of the enzyme in the given form. [e] The unprotonated PLP from of *E. coli* AATase. [f] From Goldberg *et al.* (1991). [g] The protonated PLP form of *E. coli* AATase. [h] Based on the complex of E (pig cytosolic AATase) and β-HO-Asp (L-*erythro*-β-hydroxyaspartate) (Metzler & Metzler, 1987). [i] The PMP form *E. coli* AATase under conditions similar to those given above, with 10 mM L-cysteine sulfinate.

was matched.[3] Varying the microscopic rate constants indirectly *via* their associated Gibbs free-energy levels enhanced computational performance since it required that a pair of microscopic rate constants was varied at a constant ratio for each iteration. The calculations were based on 1 mM substrate concentrations (≫[E]), and the free-energy barriers for the bimolecular steps were constrained to ≤12 kcal mol^{-1} (≥10^7 M^{-1} s^{-1}). The free-energy level of the L-Asp + E-PLP mixture was arbitrarily fixed at 0 kcal mol^{-1}, and that of the OAA + E-PMP mixture was set to 3.1 kcal mol^{-1} = $-RT$ ln(K_{eq}^{half}), where K_{eq}^{half} is the experimentally determined equilibrium constant for the half-reaction (see Appendix), and T = 298 K. On the basis of spectroscopic data (Results), the free-energy level of EL·A was constrained to equal that of EA. Equilibrium isotope effects were fixed at 1, except for the 1,3 prototropic shift where the abstracted hydron significantly washes out in competition with the reverse reaction (Julin *et al.*, 1989). The solvent D_2O viscosity effects on the association and dissociation rate constants were held at 1.22 on the basis of the relative viscosity of D_2O at 25 °C (Matsunaga & Nagashima, 1983; Weast, 1979). Altogether, five barrier and three ground state free-energy levels were varied. The simulation was repeated more than 10 times using different initial values to increase the probability that the calculated set of microscopic rate constants represents a global minimum. The barrier (varied from 10 to 20 kcal mol^{-1}) and the intermediate (from 0 to 2 kcal mol^{-1}) values were initially set equal to each other. All simulations gave the same result except that the transaldimination barrier height and to a lesser extent the free-energy level of EM·O could not be defined as noted in the Discussion section.

RESULTS

Absorbance Spectrum of the AATase-L-Asp-OAA Complex. The spectrum of AATase in the presence of saturating concentrations of L-Asp and OAA is shown in Figure 1. This spectrum resembles those of pig cytosolic and chicken mitochondrial AATase with the same pair of substrates (Metzler & Metzler, 1987; Malashkevich *et al.*, 1993). The spectrum was fitted to the sum of lognormal distribution functions in order to resolve the extinction coefficients of the overlapping bands (Johnson & Metzler, 1970; Metzler *et al.*, 1988). The band parameters are given in Table 2. Peak heights rather than areas were used to calculate relative intermediate concentrations because the former values are less sensitive to light scattering.

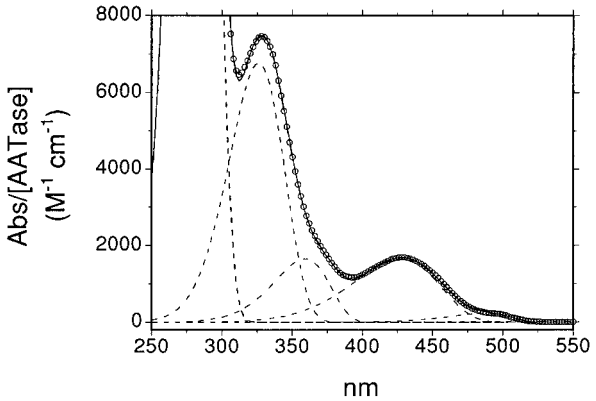

FIGURE 1: Spectrum of 38 μM wild-type aspartate aminotransferase in the presence of 38 mM L-Asp, 2 mM OAA, and 0.2 M TAPS, pH 8.2, 0.1 M KCl 25 °C (○). The active sites are ≥98% occupied under these conditions (Goldberg *et al.*, 1991). The solid line shows the fit of the spectrum to the sum of five lognormal distribution functions, and the component functions are shown as dashed lines. The band parameters are listed in Table 2.

Primary KIEs with C_α ^2H-L-Aspartate and C_α ^2H-D,L-Aspartate. The Michaelis−Menten parameters of the reactions catalyzed by wild-type and Y225F AATase with C_α ^2H-L-Asp were compared to those of the reactions with the protiated substrate. Sample data are shown in Figure 2A,C, and the KIEs are given in Table 3. The C_α ^2H-L-Asp KIEs for the reaction catalyzed by Y225F are small or absent, contrasting to the larger values recorded for the reaction catalyzed by wild-type enzyme. Similar results were obtained at pH 7.5 for the racemate (Table 3).

Solvent Deuterium Kinetic Isotope Effects on Steady State Reactions Catalyzed by Wild-Type and Y225F AATase. There are significant SKIEs on the rate constants for reactions catalyzed by both wild-type and Y225F AATase (Figure 2B,D, Table 3). The solvent deuterium KIEs on k_{cat} for reactions with L-Asp catalyzed by wild-type AATase and Y225F at pH 8.4/pD 8.8 are both near 2. The SKIE on k_{cat}/K_M^{Asp} is increased from 1.3 for wild-type AATase to 2.3 for Y225F.

Solvent Deuterium Isotope Effects on the pK_a Value of the Internal Aldimine. The value of k_{cat}/K_M^{Asp} for AATase-catalyzed reactions depends on the protonation state of the

[3] A sample Excel spreadsheet is available as supporting information.

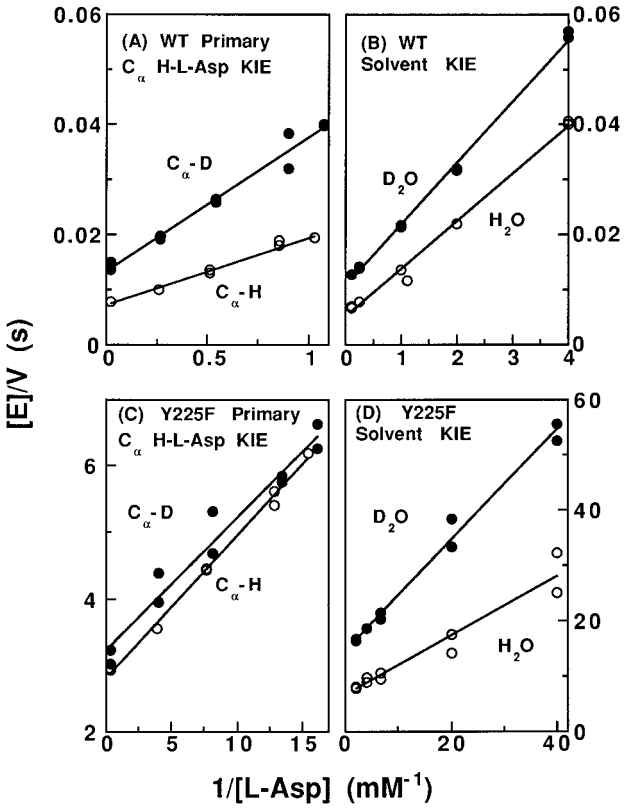

FIGURE 2: Primary C_α ^{2}H-L-Asp KIEs (A and C) and solvent deuterium KIEs (B and D) on steady state reactions catalyzed by by wild-type (A and B) and the Y225F mutant forms (C and D) of AATase with [L-Asp] varied and [αKG] ≈ 10−15 × $K_M^{αKG}$. T = 25 °C, [TAPS] = 0.2 M, I_c = 0.2 adjusted with KCl, [NADH] = 0.2 mM, and [MDH] = 2 units/mL. Reactions were monitored at 340 nm. (A) Primary C_α ^{2}H-L-Asp with 2 nM wild-type AATase, 6 mM αKG, pH = 8.90 (±0.05), 40 mM KCl. (B) Solvent D_2O KIE on reactions catalyzed by wild-type AATase as in (A) except pH = 8.40 (±0.05), pD = 8.80 (±0.05), [PMP] = 20 μM, and [KCl] = 22 mM. Experiments without added PMP gave identical results. (C) Primary C_α ^{2}H-L-Asp KIE on steady state reactions catalyzed by 1 μM Y225F with 0.1 mM αKG, pH = 8.90 (±0.05), and [KCl] = 40 mM. (D) Solvent D_2O KIEs on steady state reactions catalyzed by Y225F as in C except pD = 9.40 (±0.05) and [PMP] = 20 μM. The values of the KIEs are in Table 3.

Table 3: Primary C_α ^{2}H-(L and D,L)-Aspartate and Solvent D_2O Kinetic Isotope Effects on Steady State Reactions Catalyzed by Wild-Type and Y225F Aspartate Aminotransferase[a]

	pH	$^D(k_{cat}/K_M^{Asp})$	$^Dk_{cat}$	pH/pD	$^{D_2O}(k_{cat}/K_M^{Asp})$	$^{D_2O}k_{cat}$
WT	8.9[b]	1.9 (0.1)	1.86 (0.06)	8.4/8.8	1.3 (0.1)	1.93 (0.07)
	7.5[c]	2.4 (0.7)	1.4 (0.2)			
Y225F	8.9[b]	1.0 (0.1)	1.06 (0.04)	9.0/9.4	2.3 (0.1)	2.2 (0.2)
	7.5[c]	1.0 (0.3)	1.0 (0.1)			

[a] The reaction conditions are given in the legend to Figure 2, unless otherwise noted. Standard deviations are shown in parentheses. [b] From the data in Figure 2. [c] [D,L-Aspartate] = 0.5−20 mM (WT) or 0.5−1 mM (Y225F) after correction for the nonreacting D-enantiomer, 0.2 M HEPES; other conditions were as for pH 8.9 experiments.

internal aldimine (Kirsch *et al.*, 1984); therefore, the interpretation of the values of the SKIEs is dependent on the pK_a shifts effected by solvent substitution. The pK_a values in H_2O are 6.96 and 8.60 for wild-type and Y225F AATase, respectively (Goldberg *et al.*, 1991), and increase to 7.49 ± 0.06 and 8.97 ± 0.06, respectively, in D_2O.

Combined Primary $C_{4'}$ S ^{2}H-PMP and Solvent Kinetic Isotope Effects. The pseudo-first-order rate constants for single-turnover reactions of excess α-ketoacids with wild-type (Figure 3A) and Y225F (Figure 3B) AATase containing either $C_{4'}$ *pro-S* ^{1}H PMP or $C_{4'}$ *S* ^{2}H-PMP were measured in isotopically mixed solvents. The rate constants for reactions of both enzymes are dependent on the solvent composition. The combined KIEs on reactions of enzymes containing protiated and deuterated PMP are similar at comparable ratios of H_2O and D_2O (see Discussion).

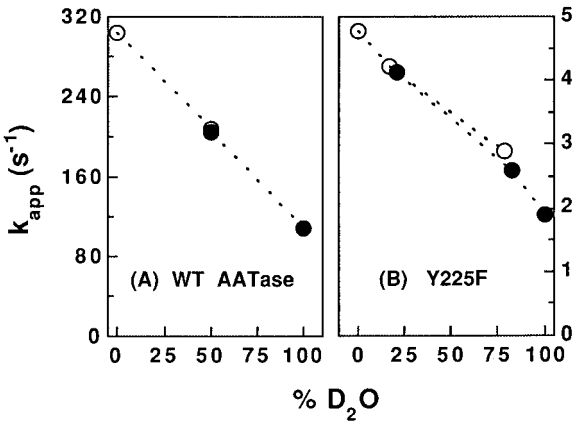

FIGURE 3: Combined primary $C_{4'}S$ ^{2}H-PMP−solvent D_2O KIEs on single-turnover half-reactions of (A) wild-type AATase with αKG and of (B) Y225F with OAA. (○) Reactions of AATase containing $C_{4'}$ *pro-S* ^{1}H-PMP (Scheme 2A,B), (●) reactions of AATase containing $C_{4'}$ *S* ^{2}H-PMP (Scheme 2C,D). Conditions: 0.1 mM α-ketoacid, 2 μM enzyme, 25 °C, 0.2 M HEPES, pH or pD = 7.50 (±0.05). The time courses were monitored at 430 nm after stopped-flow mixing. The reactions are pseudo-first-order with respect to substrate since [α-ketoacid] ≫ [E-PMP]. Furthermore, the reactions go to completion since [E] ≪ K_{half} for the reverse reactions with α-amino acids, where K_{half} is the K_M for a half-reaction. (A) $k_{app} \approx (k_{max}/k_{half}^{αKG}) \times$ [αKG], where k_{max} and K_{half} are the respective maximum rate constant and K_M value for the half-reaction, since [αKG] ≈ 0.2 × $K_{half}^{αKG}$. (B) $k_{app} \approx k_{max}$, since [OAA] ≈ 166 × K_{half}^{OAA}. The deconvoluted KIEs are given in Table 5.

Solvent Viscosity Effects. Solvent viscosity effects on k_{cat}/K_M and on k_{cat} may measure the extent to which a reaction is diffusion controlled (Brouwer & Kirsch, 1982). The normalized expression for the dependence of $1/(k_{cat}/K_M^{Asp})$ on solvent relative viscosity (η/η^0) is given in eq 1

$$(1/k_{cat}/K_M^{Asp})_{norm} = (k_{cat}/K_M^{Asp})\eta^0/(k_{cat}/K_M^{Asp})\eta = \alpha(k_{cat}/K_M^{Asp})\eta^0\alpha(\eta/\eta^0) + \beta(k_{cat}/K_M^{Asp})\eta^0 \quad (1)$$

where $(k_{cat}/K_M^{Asp})_{\eta^0}$ is the value of k_{cat}/K_M^{Asp} in the absence of added viscosogen, $(k_{cat}/K_M^{Asp})_\eta$ is the value of k_{cat}/K_M^{Asp} in the presence of viscosogen, and α and β are, respectively, the slope and intercept terms, defined in terms of microscopic rate constants in eq A4 of the Appendix.

The normalized viscosity dependence of $1/k_{cat}$ for the forward (L-Asp to L-Glu direction) transamination reaction is given by eq 2

$$(1/k_{cat})_{norm} = (k_{cat})\eta^0/(k_{cat})\eta = (k_{cat})\eta^0(\alpha_{k_{Asp}} + \alpha_{k_{αKG}})(\eta/\eta^0) + (k_{cat})\eta^0(\beta_{k_{Asp}} + \beta_{k_{αKG}}) \quad (2)$$

where $(k_{cat})_{\eta^0}$ is the value of k_{cat} in the absence of added viscosogen, $(k_{cat})_\eta$ is the value in the presence of viscosogen.

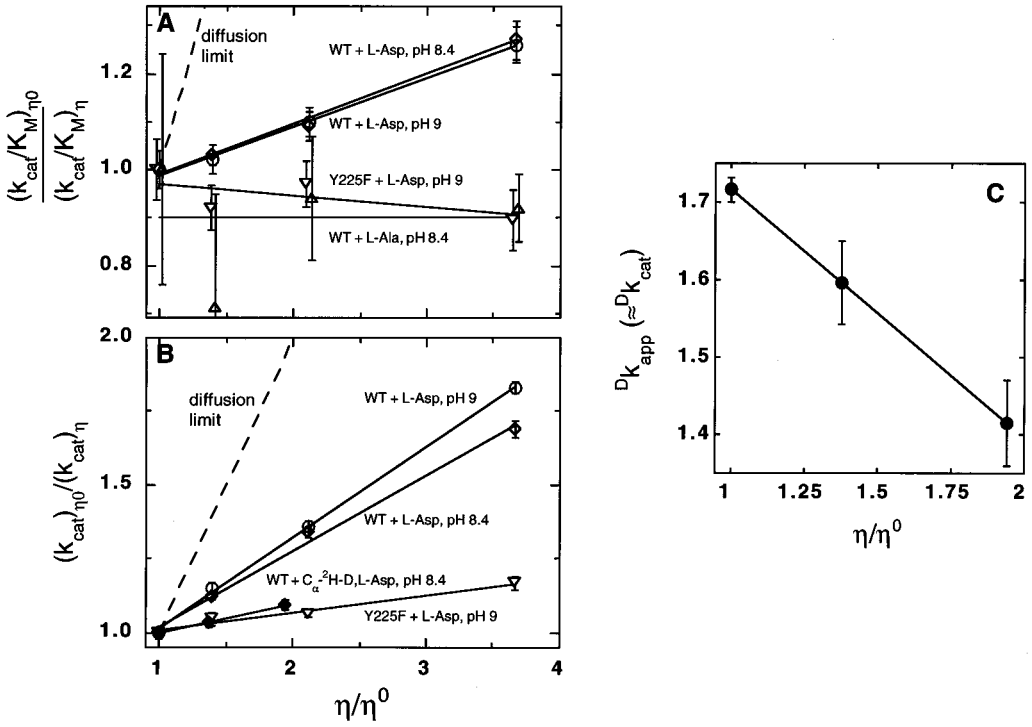

FIGURE 4: The sucrose-mediated solvent viscosity effects on the kinetic parameters of steady state reactions catalyzed by wild-type AATase and Y225F with the indicated substrate plus [αKG] ≥ 5 × $K_M^{αKG}$. (A) The ratio of the value of k_{cat}/K_M at $η^0$ (no sucrose added) to that at increased viscosity, as a function of the relative viscosity, $η/η^0$. The values of some data are offset by −0.02 (for Y225F + L-Asp) or +0.02 (for WT + L-Ala) to prevent the overlap of error bars. (B) The ratio of k_{cat} at $η^0$ to that at viscosity $η$ as a function of $η/η^0$, unless otherwise noted. The concentrations of $C_α$ ^{2}H-D,L-Asp and αKG were saturating in that experiment; therefore, $v/[E] ≈ k_{cat}$. Symbols: (○) wild-type (WT) AATase with L-Asp, pH 9; (◇) WT with L-Asp, pH 8.4; (▽) Y225F with L-Asp, pH 9; (△) WT with L-Ala, pH 8.4; (◆) WT with $C_α$ ^{2}H-D,L-Asp, pH 8.4. Other experimental conditions are given in the footnotes of Table 4. The solid lines are weighted linear fits of eq 1 (= eq A6) to the data in panel A and of eq 2 to the data in panel B. The slopes of the lines, *i.e.*, the viscosity effects, are given in Table 4. (C) The effect of increased solvent viscosity on the KIE for the AATase-catalyzed reaction with 25 mM $C_α$ ^{2}H-D,L-aspartate. The conditions were as described in the legend of Figure 2, except that the pH was 8.4. $v/[E] ≈ k_{cat}$.

$α_{k_{Asp}}$, $α_{k_{αKG}}$, $β_{k_{Asp}}$, and $β_{k_{αKG}}$ are the slope and intercept terms defined in eq A5 (see Appendix), where the subscripts k_{Asp} and $k_{αKG}$ indicate that the slope or intercept term is composed of microscopic rate constants from half-reactions starting with L-Asp or αKG, respectively. The viscosity dependencies of the kinetic parameters for other substrates may be derived by symmetry. The general forms of eqs 1 and 2 are independent of the number of reaction intermediates interconverting by first-order processes.

The reciprocal values of the kinetic parameters for the transamination reaction are linearly dependent on $η/η^0$, as seen for other enzyme-catalyzed reactions (Brouwer & Kirsch, 1982; Blacklow *et al.*, 1988; Stone & Morrison, 1988; Tipton, 1993). The normalized slope term values vary from 0, at which value the overall reaction rate is chemistry limited, to 1, where the reaction is fully diffusion controlled.

The values of $(k_{cat}/K_M^{Asp})_{η^0}/(k_{cat}/K_M^{Asp})_η$ and $(k_{cat})_{η^0}/(k_{cat})_η$ for reactions catalyzed by wild-type AATase and Y225F are plotted against sucrose-mediated $η/η^0$ in Figure 4A,B. The normalized slope terms from weighted linear regression analyses of the data in Figure 4, referred to as viscosity effects, are given in Table 4. The largest viscosity effects are on k_{cat} for the wild-type-AATase-catalyzed reaction of the L-Asp-αKG substrate pair (Figure 4B). There is also significant dependence on viscosity for k_{cat}/K_M^{Asp} (Figure 4A; Table 4), k_{cat}/K_M^{OAA}, and k_{cat} for the OAA-L-CS substrate pair (Table 4). The effect on k_{cat} for the Y225F-catalyzed reaction of L-Asp (Figure 4B) is small, and k_{cat}/K_M is viscosity independent for the slow reactions catalyzed by wild-type AATase with L-Ala, and Y225F with L-Asp (Figure 4A). There is also no effect on the velocity of the slow reaction catalyzed by the N194L mutant of AATase.[4] The value of the primary $C_α$ ^{2}H D,L-Asp KIE on wild-type-AATase-catalyzed reactions in the presence of saturating substrates decreases as a function of $η/η^0$ (Figure 4C). The complex of AATase with the competitive inhibitor maleate serves as a model for the Michaelis complexes. The K_d value at pH 8.4 in 0.2 M TAPS, 25 °C is 40 ± 3 mM at both $η/η^0 = 1$ and $η/η^0 = 3.6$.

DISCUSSION

Spectrophotometrically Determined Internal Equilibria. The relative populations (Table 2, last column) of the spectroscopically identifiable intermediates in *E. coli* AATase-catalyzed transamination were calculated from the electronic absorption spectrum of the binary complex with L-Asp and OAA (Figure 1). The species absorbing at 355 and 421 nm were respectively assigned to EL·A and EA (Scheme1), on the basis of the assignment of these peaks in the αMeAsp complex (Deng *et al.*, 1993). They each comprise about 20% of the total population (Table 2); therefore, the internal equilibrium constant for transaldimination K_{trans} = [EA]/[EL·A] = k_{23}/k_{32} = 1 (see eq A1 in the Appendix for

[4] The limiting steady kinetic parameters for N194L based on measurements at 25 °C and 0.2 M TAPS, pH 9, 40 mM KCl, were calculated from eq 4a from Goldberg *et al.* (1991), assuming lower and upper pK_a values of 8.34 and 9.7, respectively. The results are k_{cat}/K_M^{Asp} = 470 M^{-1} s^{-1}, k_{cat} = 2.5 s^{-1}, and K_M^{Asp} = 5.3 mM.

Table 4: Sucrose-Induced Solvent Viscosity Effects on Steady State Reactions Catalyzed by Wild-Type, Y225F, and N194L Aspartate Aminotransferases (AATase)[a]

varied substrate[c]	fixed substrate[d]	pH	solvent viscosity effect[b] k_{cat}/K_M (SE)	solvent viscosity effect[b] k_{cat} (SE)
wild-type AATase[e]				
L-Asp[f]	αKG	9.0	0.102 (0.005)	0.305 (0.005)
L-Asp[f]	αKG	8.4	0.104 (0.008)	0.26 (0.02)
C_α ^{2}H-Asp[f,g]	αKG	8.4		0.100 (0.006)
OAA	L-CS	8.4	0.23 (0.01)	0.22 (0.02)
αKG	L-Asp	8.4	−0.12 (0.04)	0.148 (0.001)
L-CS[h]	αKG	8.4	−0.04 (0.02)	0.10 (0.01)
L-Ala[f,h,i]	αKG	8.4	0.00 (0.04)	
Y225F[f,j]				
L-Asp	αKG	9.0	−0.02 (0.02)	0.060 (0.007)
N194L[k]				
L-Asp[k]	αKG[k]	8.4		−0.05 (0.05)

[a] 25 °C, 0.2 M TAPS, $I_c = 0.2$ adjusted with KCl. 4 units of malate dehydrogenase/mL (unless otherwise noted) and 0.2 mM NADH were added to couple the reaction. Relative viscosities (η/η^0) were from 1 to ~4, corresponding to sucrose concentrations of 0−1 M. [b] The values reported are the slopes of plots of the ratio of the kinetic parameter in the absence of sucrose (viscosity = $\eta 0$) to that in the presence of sucrose (viscosity = η), against $\eta/\eta 0$ (*e.g.*, Figure 4 and eqs 1, A6, and 2). A solvent viscosity effect of 0 indicates that the rate constant is fully chemistry controlled, and a value of 1 is indicative of a fully diffusion-limited reaction. [c] The concentration of this substrate was varied from 0.5 to 5 × K_M unless otherwise noted. [d] The concentration was ≥5 × K_M. [e] [AATase] = 2 nM. [f] Data from Figure 4. [g] [C_α ^{2}H-D,L-Asp] = 20 mM (5 × K_M). [h] The coupling enzyme was 20 units of lactate dehydrogenase/mL. [i] [L-Alanine] = 100−500 mm. [j] [Y225F] = 1 μM. [k] [N194L] = 1 μM, [L-Asp] = 100 mM, [αKG] = 30 mM, 5× their respective K_M values for this mutant.

subscript definitions). The concentration of the quinonoid form was estimated as 1.1% from the absorbance at 482 nm (Metzler & Metzler, 1987). The ketimine, *gem*-diamine, and carbinolamine intermediates as well as the OAA·E-PMP complex absorb at or near 323 nm, and their combined concentration of 74% was calculated from the extinction coefficient of the PMP form of AATase. The estimated relative concentrations of these entities are very similar to those observed for AATase complexes from other species (Metzler & Metzler, 1987; Malashkevich *et al*., 1993).

The relative populations of the intermediates absorbing near 323 nm cannot be determined from these data alone; it is useful, however, to define the equilibrium constant, $K_{1,3}$, separating EA (λ_{max} = 421 nm) from K and EM·O (λ_{max} = 323 nm) (eq 3).

$$K_{1,3} = ([K] + [EM{\cdot}O])/[EA] \quad (3a)$$

$$= k_{34}/k_{43}(1 + k_{45}/k_{54}) \quad (3b)$$

The 1,3 subscript indicates that the intermediates absorbing at 421 and 323 nm are separated by the 1,3 prototropic shift. Equation 3a can be expressed in terms of the microscopic rate constants defined in eq A1 by factoring [K] from the numerator and applying the relationships $[K]/[EA] = k_{34}/k_{43}$ and $[EM{\cdot}O]/[K] = k_{45}/k_{54}$. The result is eq 3b. Using the values from Table 2, $K_{1,3} = 0.74/0.2 = 3.7$.

C_α ^{2}H-L (and D,L*)-Aspartate Primary Hydrogen Kinetic Isotope Effects*. The C_α-KIEs for wild-type-AATase-catalyzed transamination (Figure 2A; Table 3), indicate that C_α proton abstraction is at least partially rate-determining for this reaction. The absence of primary C_α-KIEs on reactions catalyzed by Y225F clearly indicates that C_α-proton abstraction is not rate-determining for the reactions catalyzed by this mutant (Figure 2C, Table 3).

Solvent Kinetic Isotope Effects on Steady-State Reactions. The SKIEs on the steady state parameters for reactions of wild-type AATase and Y225F (Figure 2B, Table 3) indicate that a step (or steps) involving the transfer of a proton in rapid equilibrium with solvent is partially rate-determining. A fraction of the effect on wild-type enzyme may also be due to reactant diffusion since the viscosity of D_2O is 1.22-fold that of H_2O at 25 °C (Matsunaga & Nagashima, 1983; Weast, 1979). The SKIEs on k_{cat}/K_M^{Asp} may involve trans-aldimination or ketimine hydrolysis. The latter process is the more likely candidate since model transimination reactions are more facile than the corresponding transaldiminations (Jencks & Cordes, 1963). The SKIE could also result from protonation of the $C_{4'}$ atom of the quinonoid intermediate. The source of the SKIE on k_{cat} may involve any combination of these steps as well as a contribution from the αKG-to-L-Glu half-reaction.

A step subsequent to C_α H abstraction cannot be ruled out as a primary rate-determining step for wild-type AATase on the basis of the small value of $^{D_2O}k_{cat}/K_M^{Asp}$ because the rate constant for replacing a hydron on the C_α carbanion by deuterium is less than that by hydrogen. The presence of deuterium, therefore, decreases the probability that K will reform EA, offsetting the effect of a reduction of the rate of the subsequent steps on k_{cat}/K_M^{Asp}. This factor is evaluated quantitatively below.

Deconvolution of the Primary $C_{4'}$ S ^{2}H PMP and Solvent Kinetic Isotope Effects on Reactions of E-PMP with α-Ketoacids. The primary $C_{4'}$ *S* ^{2}H PMP kinetic isotope effect measures the extent to which $C_{4'}$ *pro-S* proton abstraction is rate-determining for an α-ketoacid-to-L-amino acid half-reaction. This KIE cannot be measured by multiple-turnover methods since the $C_{4'}$ *S* PMP deuterium atom is released in the first turnover. It is also difficult to measure this KIE in single-turnover reactions in H_2O due to rapid enzyme-catalyzed exchange of the $C_{4'}$ *S* atom (Kochhar *et al*., 1987; Tobler *et al*., 1987). Therefore, the combined primary $C_{4'}$ *S* ^{2}H PMP KIE/SKIE was measured in mixed solvent, such that the deuterated enzyme−cofactor complex was not exposed to H_2O until the reactions were initiated by mixing in a stopped-flow spectrometer (Scheme 2, Figure 3). The primary $C_{4'}$ *S* ^{2}H PMP KIE and SKIE were deconvoluted as follows: The difference in the rate constants for single-turnover reactions of enzyme containing $C_{4'}$ *pro-S* ^{1}H-PMP and $C_{4'}$ *S* ^{2}H-PMP in similar D_2O concentrations, Δk, is the difference in the rate constants measured in Scheme 2 panels B and C. The primary $C_{4'}$-KIE = $k_H/(k_H - \Delta k)$, where k_H is the rate constant for the reaction of enzyme containing [4′ *pro-S* ^{1}H]-PMP in 100% H_2O (Scheme 2A). The SKIE = $k_H/(k_D + \Delta k)$, where k_D is the rate constant for [4′ *S* ^{2}H]-PMP enzyme in 100% D_2O (Scheme 2D). The calculated $C_{4'}$ KIEs and SKIEs are given in Table 5.

The value of $\Delta k \approx 0$ (Figure 3), so the primary $C_{4'}$ KIEs are nearly unity for the reactions of both wild-type and Y225F AATase with α-ketoacids (Table 5). Therefore, $C_{4'}$ *pro-S* proton abstraction is not rate-determining for either reaction.

Solvent Viscosity Effects. The sucrose-induced decrease in the kinetic parameters of the wild-type *E. coli* AATase reaction with its preferred substrates (Figure 4; Table 4) may

Table 5: Primary $C_{4'}$ *S* ^{2}H-PMP and Solvent Kinetic Isotope Effects on Half-Reaction Rate Constants for Wild-Type and Y225F AATase with α-Ketoacids[a]

reaction	$^{C_{4'}\ S\ ^2H\text{-}PMP}k_{app}$	$^{D_2O}k_{app}$
WT AATase + αKG[b]	1.0 (0.2)	2.8 (0.3)
Y225F + OAA[c]	1.1 (0.2)	2.5 (0.1)

[a] The kinetic isotope effects are calculated from data shown in Figure 3 as described in the Discussion and Scheme 2. The conditions are given in the Figure 3 legend. [b] k_{app} is approximately equal to $k_{cat}/K_M^{\alpha KG} \times [\alpha KG] = 0.1\ mM = 0.2 \times K_M^{\alpha KG}$. [c] k_{app} is approximately equal to k_{OAA}, since the [OAA] of 0.1 mM is $170 \times K_M^{OAA}$ for the half-reaction (J.M. Goldberg and J.F. Kirsch, manuscript in preparation).

be assigned to a true viscosity effect on the basis of several criteria: The dissociation constant for the maleate complex (Results), and the value of k_{cat}/K_M for the slowly reacting substrate L-Ala (Figure 4; Table 4) are both independent of the sucrose concentration. The cosolute effects on reactions catalyzed by slowly reacting mutant AATase forms Y225F and N194L[4] are small or undetectable (Table 4). Controls with slowly reacting substrates and mutant enzymes, while valuable, may mislead if their rate-determining chemical step-(s) differ from those for the wild-type catalyzed reaction with the preferred substrate. By contrast, the viscosogen effect on the primary KIE on the reaction catalyzed by wild-type enzyme with a preferred substrate probes specifically the effect of the cosolute on an isotope-sensitive chemical step (Tipton, 1993; Sampson & Knowles, 1992). Increasing viscosity reduces the value of the KIE on wild-type-AATase catalyzed reactions of saturating concentrations of [α-^{2}H]-D,L-aspartate and αKG (Figure 4C); therefore, the viscosogen raises a kinetic barrier distinct from C_α proton abstraction. Taken together, the above considerations indicate that the rate of the wild-type-AATase-catalyzed transamination is partially diffusion controlled.

Assignment of the Viscosity Effect to OAA Dissociation. In principle, the barriers for association of any of the four reactants, L-Asp, OAA, αKG, and L-Glu, could contribute to the viscosity effects reported in Figure 4 and Table 4. However, the rate constant for the dissociation of OAA is probably responsible for most of the observed viscosity effect. The largest bimolecular rate constant for any AATase substrate is $k_{cat}/K_M^{OAA} = 2 \times 10^7\ M^{-1}\ s^{-1}$ (Kuramitsu *et al*., 1990). This figure approaches the diffusion limit for enzymatic rate constants (Fersht, 1985). The macroscopic rate constants for k_{cat}/K_M^{Asp}, k_{cat}/K_M^{OAA} and k_{cat} contain the microscopic rate constant for the dissociation of OAA (Appendix, eqs A4 and A5) and are sensitive to viscosity (Table 4), while that for $k_{cat}/K_M^{\alpha KG}$, which lacks the OAA dissociation rate constant, does not decrease with increasing viscosity (Table 4).

Although the qualitative conclusion derived from the viscosity variation data that OAA dissociation is largely responsible for the sensitivity of the macroscopic rate constants to viscosity is secure, quantitative interpretation is limited by specific secondary effects due to the high concentration of sucrose [see Bazelyansky *et al*. (1986)]. In the present work, the value of $k_{cat}/K_M^{\alpha KG}$ is slightly increased with increasing sucrose concentration, and an effect on the apparent equilibrium constant for the L-Asp-to-OAA half-reaction is indicated by the unequal effects of added sucrose on the two k_{cat}/K_M values.

Minimal Mechanism for Wild-Type AATase-Catalyzed Transamination. The initial step in delineating the free-energy profile for the L-Asp-to-OAA half-reaction is to identify a minimum set of intermediates consistent with the available data (eq A1). The spectrum of the enzyme−reactant complex (Figure 1, Table 2) provides evidence for the existence of the E-PLP·L-Asp Michaelis complex (355 nm), the external aldimine intermediate (421 nm), and intermediates absorbing near 330 nm, possibly including the *gem*-diamine, ketimine, and carbinolamine intermediates and the non-covalent E-PMP·OAA complex. No significant 330 nm absorbance is present in the electronic absorption spectrum of the αMeAsp−AATase complexes (Fasella *et al*., 1966; Goldberg *et al*., 1991) indicating that the *gem*-diamine intermediate is not populated. It is not known if this finding extends to the L-Asp complex, but the remainder of this analysis is predicated on this assumption. Two intermediates absorbing near 330 nm are required to accommodate the entire set of experimental kinetic and equilibrium parameters in the construction of the free-energy profile. One of these is probably the ketimine intermediate which predominates in cocrystals of AATase with reactants (Malashkevich *et al*., 1993). The solvent viscosity effect on OAA dissociation suggests that the second is the Michaelis−Menten complex with OAA. Rate constants involving the carbinolamine intermediate and domain motions (Malashkevich *et al*., 1993) may contribute significantly to the kinetics; these four intermediates (EL·A, EA, K, and EM·O), however, with Q off-pathway or present on-pathway in small amounts, are sufficient to explain the available data.

Free-Energy Profile for the L*-Asp-to-OAA Half-Reaction of Wild-Type AATase.* A set of microscopic rate constants (defined in eq A1) and intrinsic KIEs was found that is consistent with the 11 experimentally determined kinetic and equilibrium parameters collected in Table 6. The values of the microscopic parameters are given in Table 7, and the calculated and experimental parameters are compared in Table 6. The free-energy profile calculated from the microscopic parameters is shown in Figure 5A. The robustness of the calculated solution was tested by independently reducing the heights of each of the kinetic barriers in Figure 5A by 1 kcal mol^{-1}, or increasing the free-energy levels of the intermediates by the same quantity, and calculating the effects on the macroscopic parameters (Table 8). Reductions of the barriers for the EL·Asp complex and external aldimine formation did not affect the value of any macroscopic parameter by more than 5%; therefore, these barrier heights are not determined; however, the equilibrium constant for transaldimination is established spectroscopically (Table 2). Changes in the remaining barriers affect at least one macroscopic parameter by >70%, indicating that their free energies of activation are well determined by the data. Changes in the free-energy levels of intermediates, except for that of EM·O, result in large changes in $K_{1,3}$ (Table 8, column 8); therefore, the free-energy levels of the intermediates except for that of EM·O are well determined.

The simulation was run automatically with a wide variety of initial estimates of the Gibbs free-energy levels of the kinetic barriers and intermediates in order to uncover correlations giving alternative solutions (see Materials and Methods). No other set of free-energy levels was found; therefore, with the exceptions noted above, the microscopic rate constants are well determined and limited only by the

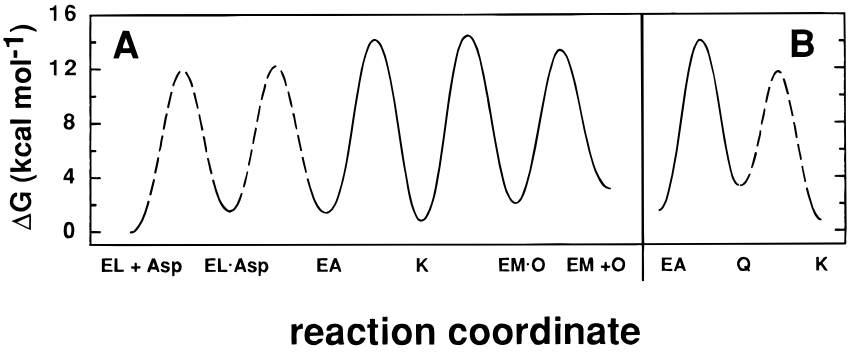

FIGURE 5: (A) Calculated free-energy profile of the L-Asp-to-OAA transamination half-reaction of wild-type *E. coli* AATase at 25 °C, pH ≈ 8.0 and [L-Asp] = [OAA] = 1 mM ≫ $[E]_t$. The values of the microscopic rate constants from Table 7 were converted to free energies using the Eyring equation (Segel, 1993). The free energies of the barriers represented by the dashed curve were not determined and are lower than those indicated by the solid curve. (B) Alternative free-energy profile for the 1,3 azaallylic proton transfer with the quinonoid intermediate on-pathway.

Table 6: Comparison of Experimental Kinetic Parameters for Reactions Catalyzed by Wild-Type *E. coli* AATase to Those Calculated from the Microscopic Rate Constants and Intrinsic Kinetic Isotope Effects in Table 7[a]

parameter	value[b]	C_α KIE[c]	SKIE[d]	solvent viscosity effect[e]
k_{cat}/K_M^{Asp}	expt 1.03×10^5 M^{-1} s^{-1}	2.4	1.3	0.104
	calcd 1.03×10^5 M^{-1} s^{-1}	2.4	1.3	0.104
k_{Asp}	expt 314 s^{-1}	1.61		
	calcd 314 s^{-1}	1.68	2.42[f]	0.13[f]
k_{cat}/K_M^{OAA}	expt 2.06×10^7 M^{-1} s^{-1}			0.23
	calcd 2.06×10^7 M^{-1} s^{-1}		2.39[f]	0.104
k_{OAA}[h]	expt 800 s^{-1}			
	calcd 800 s^{-1}		2.37[f]	0.00[f]
$K_{1,3}$[g]	expt 3.7			
	calcd 3.7			
K_{trans}[h]	expt 1			
	calcd 1			

[a] The calculation methods are described in Materials and Methods. The equations are given in Table 1, and the calculated entries were constrained by experimental data, except where noted. [b] Unless noted otherwise, the experimental values in this column are from Kuramitsu *et al*. (1990) and modified as described in the Appendix. [c] The experimental values of $^Dk_{cat}/K_M^{Asp}$ are from Table 3. The value of $^Dk_{Asp}$ was calculated from $^Dk_{cat}$ (Table 3) as described in the Appendix. [d] The experimental values are from Table 3. [e] A measure of the extent to which the reaction is diffusion limited. The experimental values are from Table 4. [f] These values were not subject to constraint because the experimental values are not available. [g] The internal equilibrium constant, ([K] + [EM·O])/[EA], for the enzyme−substrate complex (Table 2). [h] The internal equilibrium constant for transaldimination, [EA]/[EL·A], from the relative populations in the enzyme−substrate complex (Table 2).

Table 7: Microscopic Rate Constants and Intrinsic Isotope Effects for the L-Asp-to-OAA Half-Reaction Catalyzed by Wild-Type *E. coli* AATase

rate constant[a]	reacting species[a]	value[b]	intrinsic isotope effects	
			C_α KIE[c]	SKIE[d]
k_{12} M^{-1} s^{-1}	EL + A	1.50×10^7	1	1.22
k_{21} s^{-1}	EL·A	1.92×10^5	1	1.22
k_{23} s^{-1}	EL·A	1.04×10^5[f]	1	2.58
k_{32} s^{-1}	EA	1.04×10^5	1	2.58
k_{34} s^{-1}	EA	3.70×10^3	2.43	1
k_{43} s^{-1}	K	1.12×10^3	1	2.43
k_{45} s^{-1}	K	7.28×10^2	1	3.93
k_{54} s^{-1}	EM·O	5.72×10^3	1	3.93
k_{56} s^{-1}	EM·O	3.20×10^4	1	1.22
k_{65} M^{-1} s^{-1}	EM + O	2.13×10^8	1	1.22

[a] The microscopic rate constants and the reacting species are defined in eq A1 in the Appendix. [b] This set of microscopic rate constant values represents the best fit to the set of experimental parameters for wild-type AATase collected in Table 6, with the exceptions discussed in the text. The microscopic rate constants were varied during the minimization procedure and subject to constraints as described in the Materials and Methods. The free-energy profile calculated from the microscopic rate constants is shown in Figure 5A. [c] Only the intrinsic isotope effects for k_{34} and k_{43} in this column were varied. [d] The equilibrium isotope effects = 1, except for C_α proton abstraction.

quality of the data, and the untested assumption that the C_α deuteron of L-Asp is exchanged with solvent more rapidly than OAA formation.[5] The estimates of the intrinsic solvent KIE values on transaldimination and ketimine hydrolysis varied among simulations, indicating that these values are uncertain.

The data and calculations presented in Figure 5A and Tables 6−8 define quantitatively the free-energy profile for the *E. coli* AATase. The rate-determining step for the wild-type enzyme in the L-Asp-to-OAA direction is predominantly ketimine hydrolysis, and ketimine formation is rate-determining in the OAA-to-L-Asp direction at low [OAA] (k_{cat}/K_M^{OAA} conditions), as required by microscopic reversibility. On the other hand, the relative stability of the ketimine makes the 1,3 azaallylic shift rate-determining at saturating [OAA] (k_{OAA} conditions).

Is the Quinonoid Species on or off the Main Reaction Pathway? The 1,3 prototropic shift appears to be concerted for pig cytosolic AATase, bypassing the carbanion intermediate, with the quinonoid species forming off the main reaction pathway (Julin & Kirsch, 1989). This interpretation is supported by the earlier observation that the quinonoid species appears before the rate-determining step of transamination (Fasella & Hammes, 1967). The calculated value of the intrinsic C_α KIE of 2.43 for *E. coli* AATase is only half of that of the measured value in the chemical rescue of the K258A transamination reaction of L-Asp (Toney & Kirsch, 1992). The lower result calculated here implies a different transition state for the two reactions and suggests that, like the reaction of pig cytosolic AATase with L-Asp, the reaction catalyzed by *E. coli* AATase proceeds through a bent rather than a linear transition state (Chart 1) in a concerted 1,3 prototropic shift. The barrier for $C_{4'}$ proton abstraction is small on the basis of the absence of a $C_{4'}$ KIE (Table 5); therefore, the transfer of the C_α and $C_{4'}$ protons may be

[5] The ratio of the respective rate constants for washout of ^2H from C_α ^2H-L-Asp and OAA formation is 2.6 for pig cytosolic AATase (Julin *et al*., 1989).

Table 8: Free-Energy Levels of the Kinetic Barriers and Intermediates for the L-Asp-to-OAA Half-Reaction for Wild-Type AATase. Sensitivity of the Macroscopic Parameters to Changes in the Free-Energy Levels

		change (%) resulting from a 1 kcal mol^{-1} reduction in the $\Delta G^{\ddagger}$ value or from a 1 kcal mol^{-1} increase in the ΔG value for an intermediate[a]					
reaction coordinate	ΔG[b] (kcal mol^{-1})	k_{cat}/K_M^{Asp}	k_{Asp}	k_{cat}/K_M^{OAA}	k_{OAA}	k_{cat}/K_M (viscosity effect)[c]	$K_{1,3}$[d]
E-PLP + L-Asp (EL + A)	0						
L-Asp association/dissociation	11.8	1.0	*e*	0.5	1.9	−5.0	*e*
E-PLP·L-Asp (EL·A)	1.5	*f*	25	*f*	0.4	*f*	*e*
transaldimination	12.2	1.0	0.0	1.0	3.1	1.0	*e*
external aldimine (EA)	1.5	*f*	25	*f*	1.0	*f*	430
1,3 azaallyic shift	14.2	43	18	43	200	43	*f*
ketimine (K)	0.79	*f*	69	*f*	180	*f*	−73
ketimine hydrolysis/formation	14.4	73	120	73	10	73	*f*
E-PMP·OAA (EM·O)	2.1	*f*	1	*f*	20	*f*	−8.2
OAA association/dissociation	13.4	8.7	12	8.2	*e*	−74	*e*
E-PMP + OAA (EM + O)	3.1						

[a] The sign of the change for a constant indicates whether it represents an increase or decrease; the kinetic parameters are defined in Table 1. Conditions: 25 °C, pH range, 7.5−8, [L-Asp] = [OAA] = 1 mM ≫ [E]. [b] The Gibbs free-energy levels of species occurring on the reaction coordinate, which are related to the microscopic rate constants as described in the legend of Figure 5. [c] Slope term of eq 1 or A6, a measure of the extent to which the reaction is diffusion limited. [d] ([K] + [E·O])/[EA] in the enzyme−substrate complex, eq 3b. [e] The microscopic rate constant terms associated with this position on the reaction coordinate are absent from the expression for the macroscopic constant. [f] Changes in the microscopic rate constant terms associated with this position on the reaction coordinate cancel from the expression for the macroscopic constant.

Chart 1: Bent Transition State for the 1,3 Azaallylic Proton Transfer[a]

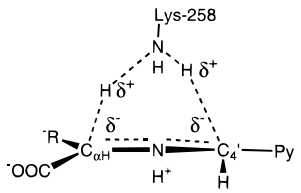

[a] $^{-}R = CH_2COO^{-}$ and Py = the substituted pyridine ring. The KIE on the $C_{4'}$ hydron transfer is very small due to the asymmetry of the transition state.

asymmetric in the concerted transition state (Chart 1), since the value of the deuterium KIE is maximal for 50% hydron transfer in the transition state (Westheimer, 1961). Thus, the spectroscopically observed quinonoid species (Table 2) probably occurs off the main reaction pathway. The quinonoid species is relatively unstable, 1.73 kcal mol^{-1} less so than the neighboring external aldimine intermediate [$-RT$ ln(fraction EA)/fraction Q], Table 2. Were the quinonoid species on the reaction pathway (Figure 5B), then an expansion of a simulated 3-intermediate mechanism to a 4-intermediate to one including Q effects a <1% change in the calculated macroscopic parameters.

Comparison to Other Transaminases. Earlier data with mitochondrial and cytosolic AATase are consistent with a mechanism in which there are several partially rate-determining steps. $K_{1,3}$ (eq 3a) is >3 for other AATases (Jenkins & D'Ari, 1966; Metzler & Metzler, 1987; Malashkevich *et al*., 1993), indicating that the ketimine intermediate is relatively stable, which supports the interpretation that conversion of this intermediate to products is relatively slow. The rates of washout of α ^{18}O from enriched α-ketoglutarate (McLeish *et al*., 1989), and C_α ^2H from amino acids (Julin *et al*., 1989) are comparable with those of the other steps in transamination, indicating the existence of one or more significant barriers after C_α H abstraction in the forward direction and after ketimine formation in the reverse direction. Although there are differences among reactions catalyzed by AATases from different sources, and even among reactions of different substrate pairs catalyzed by the same enzyme (Julin & Kirsch, 1989), the free-energy profile presented here qualitatively explains the properties of other aspartate aminotransferases.

Evolutionary Considerations. No one step is completely rate-determining in this half-reaction. Rather, the barriers for aldimine to ketimine conversion, ketimine hydrolysis and OAA dissociation are all significant. A multistep reaction with nearly equal barrier heights and intermediate stabilities is consistent with the concept of an optimized enzyme (Fersht, 1974; Cleland, 1975a; Albery & Knowles, 1976). That other steps are partially rate-determining does not imply that catalysis of the 1,3 azaallylic proton transfer has not been the focus of evolutionarily driven optimization of the enzyme. For example in the model reaction for transamination of D,L-alanine by PLP (Auld & Bruice, 1967a,b), proton transfer is the sole rate-determining step ($\Delta G^{\ddagger} = 24$ kcal mol^{-1}), and the carbonyl displacement reaction is extremely fast by comparison ($\Delta G^{\ddagger} = 18$ kcal mol^{-1}). Therefore, evolution reduced the barrier height for proton transfer by ≈6 kcal mol^{-1} relative to that for ketimine hydrolysis in order to equalize the barrier heights in the catalyzed reaction.

Ketimine Hydrolysis Is the Sole Rate-Determining Step for Y225F-Catalyzed Transamination. The kinetic data presented above show that the free-energy profile for Y225F differs significantly from that of wild-type AATase. C_α H abstraction (Table 3) and dissociation of the E-PMP·OAA complex (Table 4) are not kinetically significant. The value of the SKIE on k_{cat}/K_M^{Asp} for Y225F is larger than that value for wild-type AATase, indicating that a step involving transfer of a solvent-exchangeable proton is rate-determining for the mutant. These observations, taken together, demonstrate that ketimine hydrolysis is the rate-determining step in Y225F-catalyzed transamination. A detailed free-energy profile for Y225F and the role of Tyr-225 will be discussed further (J. M. Goldberg and J. F. Kirsch, manuscript in preparation).

ACKNOWLEDGMENT

We thank Edward Neymark for measuring many of the cosolute effects reported in Table 3, Joanne Nadherny for

the spectrum of the enzyme−substrate complex, and Dr. Lisa Gloss for a critical reading of the manuscript.

SUPPORTING INFORMATION AVAILABLE

Supporting information was created on a Macintosh IIfx computer (Apple Computer Corporation) operating with system 7.1 using Excel 4.0 and Word 5.1a (Microsoft Corporation) and SigmaPlot 4.11 (Jandel Corporation). A file created with SigmaPlot 4.11 recreates the individual and combined spectra of the AATase−substrate complex shown in Figure 1. A text file created by Word 5.1a is included describing the transform used to simulate the spectra using the parameters given in Table 2. A spreadsheet created using Excel 4.0 (Microsoft Corporation) is provided, which is similar to that used to calculate the macroscopic parameters (Table 7), the microscopic kinetic rate constants (Table 6), and the free-energy vs reaction coordinate profile (Table 8, Figure 5) from experimental data and the equations indicated in Table 1. Instruction for use of the spreadsheet is provided in a text file. See any current masthead page for access instructions.

APPENDIX

The simplest kinetic mechanism for the transamination L-Asp-to-OAA half-reaction that is consistent with the available data (see Discussion) is given by

$$\mathrm{EL} + \mathrm{A} \underset{k_{21}}{\overset{k_{12}}{\rightleftharpoons}} \mathrm{EL{\cdot}A} \underset{k_{32}}{\overset{k_{23}}{\rightleftharpoons}} \mathrm{EA} \underset{k_{43}}{\overset{k_{34}}{\rightleftharpoons}} \mathrm{K} \underset{k_{54}}{\overset{k_{45}}{\rightleftharpoons}} \mathrm{EM{\cdot}O} \underset{k_{65}}{\overset{k_{56}}{\rightleftharpoons}} \mathrm{EM} + \mathrm{O} \quad \text{(A1)}$$

where EL is E-PLP, A is L-Asp, EL·A is the Michaelis complex between EL and L-Asp, EA is the external aldimine intermediate, K is the ketimine intermediate, and EM·O is the Michaelis complex of O (OAA) and EM (E-PMP) (Scheme 1). The expressions for k_{Asp}/K_M^{Asp} and k_{Asp}, for the half-reaction shown in eq A1, were calculated by the net rate constant method (Cleland, 1975b) and are shown in eqs A2 and A3

$$k_{Asp}/K_M^{Asp} = (k_{12}k_{23}k_{34}k_{45}k_{56})/(k_{21}k_{32}k_{43}k_{56} + k_{21}k_{32}k_{43}k_{54} + k_{21}k_{32}k_{45}k_{56} + k_{21}k_{34}k_{45}k_{56} + k_{23}k_{34}k_{45}k_{56}) \quad \text{(A2)}$$

$$k_{Asp} = (k_{23}k_{34}k_{45}k_{56})/(k_{32}k_{43}k_{54} + k_{32}k_{43}k_{56} + k_{32}k_{45}k_{56} + k_{34}k_{45}k_{56} + k_{23}k_{43}k_{54} + k_{23}k_{43}k_{56} + k_{23}k_{45}k_{56} + k_{23}k_{34}k_{54} + k_{23}k_{34}k_{56} + k_{23}k_{34}k_{45}) \quad \text{(A3)}$$

Note that $k_{Asp}/K_M^{Asp} = k_{cat}/K_M^{Asp}$ for the complete reaction since k_{65} is 0 under steady state reaction conditions. The rate expressions for the other AATase substrates may be solved by symmetry and are not shown. Expressions for the effects of solvent relative viscosity (η/η^0) on K_M^{Asp}/k_{Asp} (eq A4) and $1/k_{Asp}$ (eq A5) were derived from eqs A2 and A3 by substituting each association or dissociation rate constant with the product of the rate constant and the relative viscosity, η^0/η (Brouwer & Kirsch, 1982)

$$(K_M^{Asp}/k_{Asp})_\eta = [(k_{21}k_{32}k_{43}k_{54} + k_{23}k_{34}k_{45}k_{56})/k_{12}k_{23}k_{34}k_{45}k_{56}](\eta/\eta^0) + (k_{21}k_{32}k_{43} + k_{21}k_{32}k_{45} + k_{21}k_{34}k_{45})/k_{12}k_{23}k_{34}k_{45} \quad \text{(A4)}$$

The multiplier of η/η^0 in eq A4 is defined as α in eq 1, while the intercept term is defined as β.

$$(1/k_{Asp})_\eta = [(k_{32}k_{43}k_{54} + k_{23}k_{43}k_{54} + k_{23}k_{34}k_{54} + k_{23}k_{34}k_{45})/k_{23}k_{34}k_{45}k_{56}](\eta/\eta^0) + (k_{23}k_{34} + k_{23}k_{43} + k_{23}k_{45} + k_{32}k_{43} + k_{32}k_{45} + k_{34}k_{45})/k_{23}k_{34}k_{45} \quad \text{(A5)}$$

The multiplier of η/η^0 in eq A5 is defined as $\alpha_{k_{Asp}}$ in eqs 2 and A8, while the intercept term is defined as $\beta_{k_{Asp}}$.

Equation A4 may be normalized (Brouwer & Kirsch, 1982) by multiplying by the value of k_{cat}/K_M^{Asp} in the absence of viscosogen, that is, by $(k_{Asp}/K_M^{Asp})_{\eta^0}$ (eq A2). In terms of microscopic rate constants, this is

$$(k_{Asp}/K_M^{Asp})_{\eta^0}/(k_{Asp}/K_M^{Asp})_\eta = [(k_{21}k_{32}k_{43}k_{54} + k_{23}k_{34}k_{45}k_{56})/(k_{21}k_{32}k_{43}k_{56} + k_{21}k_{32}k_{43}k_{54} + k_{21}k_{32}k_{45}k_{56} + k_{21}k_{34}k_{45}k_{56} + k_{23}k_{34}k_{45}k_{56})](\eta/\eta^0) + (k_{21}k_{32}k_{43} + k_{21}k_{32}k_{45} + k_{21}k_{34}k_{45})/(k_{21}k_{32}k_{43}k_{56} + k_{21}k_{32}k_{43}k_{54} + k_{21}k_{32}k_{45}k_{56} + k_{21}k_{34}k_{45}k_{56} + k_{23}k_{34}k_{45}k_{56}) \quad \text{(A6)}$$

Equation A6 is equivalent to eq 1, and the normalized viscosity dependence for the reverse reaction, $(k_{OAA}/K_M^{OAA})_{\eta^0}/(k_{OAA}/K_M^{OAA})_\eta$, is identical.

The value of $1/k_{cat}$ at elevated viscosity for transamination in the L-Asp-to-L-Glu direction is derived from the relationship (Velick & Vavra, 1962)

$$k_{cat} = \frac{k_{Asp}k_{\alpha KG}}{k_{Asp} + k_{\alpha KG}} \quad \text{(A7)}$$

where $k_{\alpha KG}$ is the rate constant of the half-reaction in which E-PMP and αKG are converted to E-PLP and L-Glu at saturating substrate concentrations. The value of $1/k_{Asp}$ at elevated viscosity (eq A5) and a similar expression for $1/k_{\alpha KG}$ (not shown) were substituted into eq A7, and rearrangement yields

$$(1/k_{cat})_\eta = (\alpha_{k_{Asp}} + \alpha_{k_{\alpha KG}})(\eta/\eta^0) + \beta_{k_{Asp}} + \beta_{k_{\alpha KG}} \quad \text{(A8)}$$

where $\alpha_{k_{Asp}}$ and $\beta_{k_{Asp}}$ are the respective slope and intercept terms defined above for eq A5, and $\alpha_{k_{\alpha KG}}$ and $\beta_{k_{\alpha KG}}$ are similarly defined for the αKG-to-L-Glu half-reaction. Equation A8 is normalized by multiplying by $(k_{cat})_{\eta^0}$, that is, k_{cat} at $\eta/\eta^0 = 1$, giving eq 2 in the Results section.

$^Dk_{Asp}$, the C_α ^{2}H-L-Asp KIE on k_{Asp} may be calculated from $^Dk_{cat}$, the C_α ^{2}H-L-Asp KIE on k_{cat}, and $k_{\alpha KG}$, the maximum rate of the αKG-to-L-Glu half-reaction, using eq A9 which is derived from eq A7

$$^Dk_{Asp} = {}^Dk_{cat} + (k_{Asp}/k_{\alpha KG})({}^Dk_{cat} - 1) \quad \text{(A9)}$$

The values of k_{Asp} and $k_{\alpha KG}$ used for substitution into eq A9 are discussed below.

Kinetic Parameters for Wild-Type AATase-Catalyzed Reactions Used for Construction of the Free-Energy Profile. Data from Kuramitsu *et al*. (1990) were used to calculate the steady state values for the kinetic parameters for reactions catalyzed by wild-type AATase for the sake of consistency, since that study currently contains the only report of k_{OAA} for this enzyme. The values of the steady-state parameters

were corrected by −7% on the basis of the differences in the ϵ_{280} values employed in the above study and by Goldberg *et al*. (1991). The recalculated values for k_{cat}, k_{cat}/K_M^{Asp}, and k_{cat}/K_M^{OAA} are 206 s^{-1}, 1.03 × 10^5, and 2.06 × 10^7 M^{-1} s^{-1}, respectively. The difference between the value for k_{cat} of 206 s^{-1} and that of 159 s^{-1} (Gloss & Kirsch, 1995) is probably due to differences in buffer composition. The value of K_{eq}^{half}, the equilibrium constant for the L-Asp-to-OAA half-reaction = $(k_{cat}/K_M^{Asp})/(k_{cat}/K_M^{OAA})$ = 0.005. k_{Asp} is calculated from k_{cat} and $k_{\alpha KG}$ by solving eq A7 for k_{Asp}. The recalculated value of k_{Asp} is 314 s^{-1}.

REFERENCES

Albery, W. J., & Knowles, J. R. (1976) *Biochemistry 15*, 5631−5640.

Auld, D. S., & Bruice, T. C. (1967a) *J. Am. Chem. Soc. 89*, 2083−2089.

Auld, D. S., & Bruice, T. C. (1967b) *J. Am. Chem. Soc. 89*, 2098−2106.

Bazelyansky, M., Robey, E., & Kirsch, J. F. (1986) *Biochemistry 25*, 125−130.

Blacklow, S. C., Raines, R. T., Lim, W. A., Zamore, P. D., & Knowles, J. R. (1988) *Biochemistry 27*, 1158−1167.

Brouwer, A. C., & Kirsch, J. F. (1982) *Biochemistry 21*, 1302−1307.

Cleland, W. W. (1975a) *Acc. Chem. Res. 8*, 145−151.

Cleland, W. W. (1975b) *Biochemistry 14*, 3220−3224.

Cronin, C. N., & Kirsch, J. F. (1988) *Biochemistry 27*, 4572−4579.

Danishefsky, A. T., Onuffer, J. J., Petsko, G. A., & Ringe, D. (1991) *Biochemistry 30*, 1980−1985.

Deng, H., Goldberg, J. M., Kirsch, J. F., & Callender, R. (1993) *J. Am. Chem. Soc. 115*, 8869−8870.

Fasella, P., & Hammes, G. G. (1967) *Biochemistry 6*, 1798−1804.

Fasella, P., Giartosio, A., & Hammes, G. G. (1966) *Biochemistry 5*, 197−202.

Fersht, A. (1985) *Enzyme Structure and Mechanism*, p 150, F. H. Freeman and Company, New York.

Fersht, A. R. (1974) *Proc. R. Soc. B187*, 397.

Gloss, L. M., & Kirsch, J. F. (1995) *Biochemistry 34*, 3999−4007.

Goldberg, J. M., Swanson, R. V., Goodman, H. S., & Kirsch, J. F. (1991) *Biochemistry 30*, 305−312.

Hayashi, H., Inoue, Y., Kuramitsu, S., Morino, Y., & Kagamiyama, H. (1990) *Biochem. Biophys. Res. Commun. 167*, 407−412.

Jäger, J., Moser, M., Sauder, U., & Jansonius, J. N. (1994) *J. Mol. Biol. 239*, 285−305.

Jansonius, J. N., & Vincent, M. G. (1987) in *Biological Macromolecules and Assemblies* (Jurnak, F., & Mcpherson, A., Eds.) pp 187−285, John Wiley & Sons, New York.

Jencks, W. P., & Cordes, E. (1963) in *Chemical and Biological Aspects of Pyridoxal Catalysis* (Snell, E. E., Fasella, P. M., Braunstein, A., & Rossi Fanelli, A., Eds.) pp 57−67, The Macmillan Company, New York.

Jenkins, W. T., & D'Ari, L. (1966) *J. Biol. Chem. 241*, 2845−2854.

Johnson, R. J., & Metzler, D. E. (1970) *Methods Enzymol. 18A*, 433−471.

Julin, D. A., & Kirsch, J. F. (1989) *Biochemistry 28*, 3825−3833.

Julin, D. A., Wiesinger, H., Toney, M. D., & Kirsch, J. F. (1989) *Biochemistry 28*, 3815−3821.

Kirsch, J. F., Eichele, G., Ford, G. C., Vincent, M. G., Jansonius, J. N., Gehring, H., & Christen, P. (1984) *J. Mol. Biol. 174*, 497−525.

Kochhar, S., Finlayson, W. L., Kirsch, J. F., & Christen, P. (1987) *J. Biol. Chem. 262*, 11446−11448.

Kuramitsu, S., Hiromi, K., Hayashi, H., Morino, Y., & Kagamiyama, H. (1990) *Biochemistry 29*, 5469−5476.

Malashkevich, V. N., Toney, M. D., & Jansonius, J. N. (1993) *Biochemistry 32*, 13451−13462.

Matsunaga, N., & Nagashima, A. (1983) *J. Phys. Chem. Ref. Data 12*, 933−966.

McLeish, M. J., Julin, D. A., & Kirsch, J. F. (1989) *Biochemistry 28*, 3821−3825.

Metzler, C. M., & Metzler, D. E. (1987) *Anal. Biochem. 166*, 313−327.

Metzler, C. M., Mitra, J., Metzler, D. E., Makinen, M. W., Hyde, C. C., Rogers, P. H., & Arnone, A. (1988) *J. Mol. Biol. 203*, 197−220.

Onuffer, J. J., & Kirsch, J. F. (1994) *Protein Eng. 7*, 413−424.

Sampson, N., S., & Knowles, J., R. (1992) *Biochemistry 31*, 8482−8487.

Segel, I. H. (1993) *Enzyme Kinetics*, p 937, John Wiley & Sons, Inc., New York.

Stone, S. R., & Morrison, J. F. (1988) *Biochemistry 27*, 5493−5499.

Tipton, P. A. (1993) *Biochemistry 32*, 2822−2827.

Tobler, H. P., Gehring, H., & Christen, P. (1987) *J. Biol. Chem. 262*, 8985−8989.

Toney, M. D., & Kirsch, J. F. (1989) *Science 243*, 1485−1488.

Toney, M. D., & Kirsch, J. F. (1991) *Biochemistry 30*, 7456−7461.

Toney, M. D., & Kirsch, J. F. (1992) *Protein Sci. 1*, 107−119.

Toney, M. D., & Kirsch, J. F. (1993) *Biochemistry 32*, 1471−1479.

Velick, S. F., & Vavra, J. (1962) *J. Biol. Chem. 237*, 2109−2122.

Weast, R. C. (1979) *CRC Handbook of Chemistry and Physics*, 60th ed., p F-49, Chemical Rubber Publishing Company, Boca Raton, FL.

Westheimer, F. H. (1961) *Chem. Rev. 61*, 265−273.

Yano, T., Kuramitsu, S., Tanase, S., Morino, Y., Hiromi, K., & Kagamiyama, H. (1991) *J. Biol. Chem. 266*, 6079−6085.

Yano, T., Mizuno, T., & Kagamiyama, H. (1993) *Biochemistry 32*, 1810−1815.

BI952138D